

Mechanism of heat-and-mass transfer caused by irradiation of a free melt surface by laser pulses

L.I. Antonova, A.F. Glova, S.V. Drobyazko, Yu.M. Senatorov

Abstract. The conditions for the onset and evolution dynamics of flooded jets, which were discovered for the first time upon irradiation of the free surface of melted paraffin by laser pulses, are studied experimentally. Their maximum speed and penetration depth are measured. It is shown that the initiation of flooded jets has a threshold nature and strongly affects the heat-and-mass transfer. A pattern of flows is presented, which displays the evolution dynamics of flooded jets and thermocapillary vortices in a bounded volume under repetitively pulsed irradiation of the melt surface.

Keywords: repetitively pulsed laser, flooded jet, thermocapillary vortices, heat-and-mass transfer.

1. Introduction

Studies of the regimes and properties of flows in materials melted by laser radiation is of interest for problems of laser technology, because these flows determine the heat-and-mass transfer and strongly affect the melting rate and the shape of the melt bath. This is significant for such technological processes as welding and alloying [1–4]. Closed flows in the form of thermocapillary vortices appearing under the heating of melt or liquid surfaces by cw laser radiation were investigated in papers [5–10]. The main features of unclosed flows, which appear under the action of the force of gravity and the recoil momentum of vapours during the melting of vertical metal targets by the radiation of cw and repetitively pulsed CO₂ lasers, were studied in [11–15].

This work considers another type of the flow initiated by pulsed or repetitively pulsed laser radiation on a free liquid surface. This is a flooded jet (FJ) arising near the surface and propagating normally to it into the depth. The results of an experimental study of the characteristics of this flow depending on the radiation parameters are presented.

2. Experimental

A CO₂ laser operating in a pulsed, repetitively pulsed, or a pulse-train mode was used in the experiments. Its parameters were controlled within the following ranges: the energy was $E = 0.1 - 4$ J, the pulse duration was $\tau = 20 - 120$ μ s, and the pulse repetition rate was $f = 0.1 - 300$ Hz. The laser radiation was directed vertically and focused at the free liquid surface into a spot of diameter $D = 3 - 8$ mm. The liquid filled a quartz glass cell with dimensions of 50×10 mm in the entrance plane and 50 mm high. In some cases, a bounded volume of the irradiated liquid was formed using a profiled metal strip 0.15 mm thick and 10 mm wide inserted into the upper part of the cell. The cell was illuminated by a parallel light beam. In this case, thermal inhomogeneities appearing under the action of laser radiation were detected by the shadow method, and their magnified images were projected onto a screen and recorded on a video film at a frequency of 50 Hz. The temperature of the liquid in the FJ was measured by a thermocouple with a time resolution of 0.5 ms and junction dimensions of $\varnothing 60 \times 40$ μ m. The main experiments were performed with a paraffin melt irradiated at an initial temperature $T = 60 - 100$ °C.

3. Characteristics of a FJ irradiated by single laser pulses

Fig. 1 presents typical video frames illustrating the onset and evolution of the FJ in a paraffin melt irradiated by a laser pulse with a power density $W \geq 4 \times 10^5$ W cm⁻² at the surface. At the initial stage, the FJ has a form of a cylinder with a diameter slightly smaller than the diameter of the focal spot, and as the FJ propagates, it acquires a mushroom-like shape. Simultaneously with the formation of the FJ, the liquid heated in the near-surface layer moves in a radial direction under the action of thermocapillary forces, and, after 40–60 ms after the start of the laser action, reverse flows appear at the edges of the jet, which are shown with arrows in Fig. 1 (frames 3, 4). The analysis of the video frames obtained at various E , τ , and D values has shown that, at $W = (1.2 - 4) \times 10^5$ W cm⁻², the FJ is formed as a result of a combination of several jets into a single jet, initially has a form of a truncated cone, and subsequently becomes mushroom-shaped. When the power density is below the threshold value $W_{th} \approx 10^5$ W cm⁻², no FJ appears. Note that the relaxation time τ_r of thermal perturbations increases with an increase in the pulse energy E , but its maximum value does not exceed 1 s.

L.I. Antonova, A.F. Glova, S.V. Drobyazko, Yu.M. Senatorov State Research Centre of the Russian Federation, Troitsk Institute for Innovation and Fusion Research, 142190 Troitsk, Moscow region, Russia; e-mail: svdrob@triniti.ru

Received 29 April 2002

Kvantovaya Elektronika 32 (11) 1029–1032 (2002)

Translated by A.S. Seferov

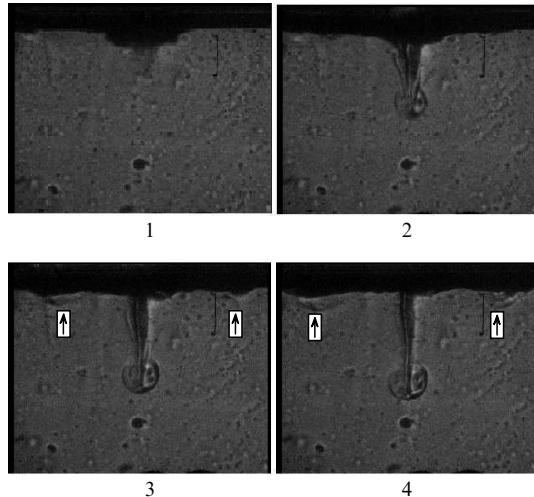


Figure 1. The onset and evolution dynamics of a flooded jet upon irradiation of a free paraffin melt surface at $T = 90^\circ\text{C}$ by a laser pulse with a power density $W = 4.2 \times 10^5 \text{ W cm}^{-2}$ ($\tau = 40 \mu\text{s}$, $E = 4 \text{ J}$, and $D = 5.5 \text{ mm}$). The time interval between the frames is 20 ms, and the first frame corresponds to a delay $t = 8 - 10 \text{ ms}$ with respect to the action of the laser pulse. Arrows indicate reverse flows.

Fig. 2 shows the dependences of the maximum depth H of the jet penetration and the maximum velocity V of the jet front motion in the paraffin melt on W at $\tau = 40$ and $70 \mu\text{s}$ and different E and D values. The velocity was determined from the two first video frames. One can see that, at $W > W_{\text{th}}$, the quantities V and H depend only on the

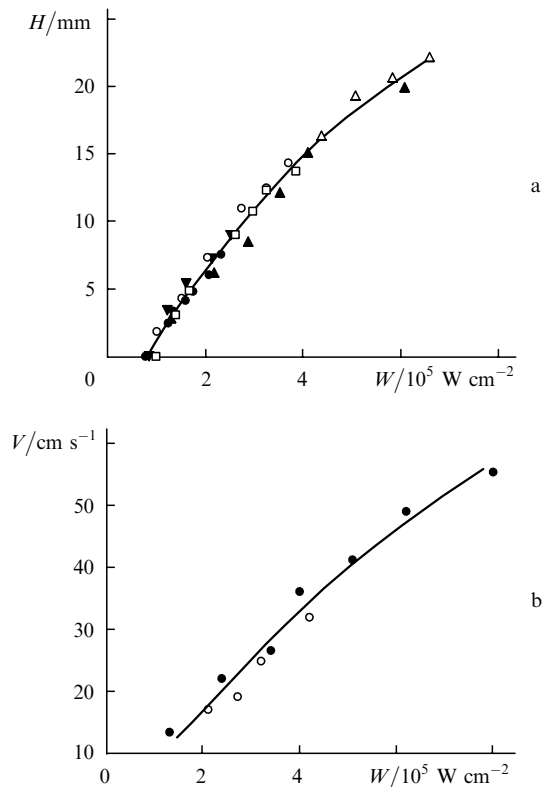


Figure 2. (a) Maximum FJ penetration depth H and (b) maximum velocity V of the FJ front motion in the paraffin melt versus the power density W . Different points correspond to different values of the parameters τ , E , and D .

power density and monotonically increase with its increase. The radial velocity of the melt motion as a function of W has a similar behaviour at $10^5 \text{ W cm}^{-2} \leq W \leq 2.2 \times 10^5 \text{ W cm}^{-2}$, and when $W > 2.2 \times 10^5 \text{ W cm}^{-2}$, this velocity stabilises at a level of $12 - 14 \text{ cm s}^{-1}$.

Fig. 3 shows time-dependent temperature changes in the FJ for three distances h between the thermocouple and surface. An abrupt temperature change by $\Delta T \approx 60^\circ\text{C}$ observed at the beginning of curve (1) for $h = 0.4 \text{ mm}$ is associated with the direct heating of the thermocouple by laser radiation. The measured dependence of this temperature increase on h made it possible to determine the laser-radiation absorption length $L = 0.4 \text{ mm}$ in the paraffin melt. At $t < 50 \text{ ms}$, two time intervals with an appreciable increase in ΔT can be additionally distinguished in curve (1). They are especially clearly pronounced in curves (2) and (3) for $h \gg L$. This character of ΔT changes testifies to a complex FJ structure and a nonuniform temperature distribution along its length. Using the known FJ parameters (the diameter and velocity) and the time dependence of ΔT for a given distance h , we can estimate the fraction of energy absorbed by the near-surface layer, which is transferred by the FJ to this distance. These estimates have shown that this fraction is $\sim 40\%$ at $h = 3 \text{ mm}$.

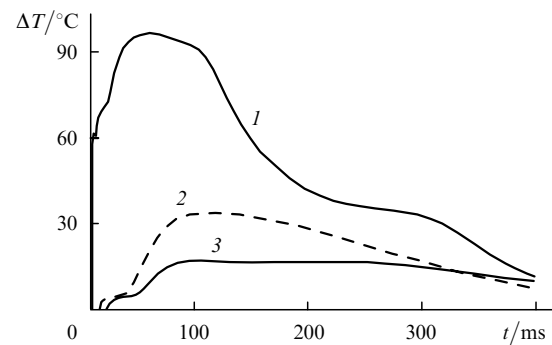


Figure 3. Time-dependent temperature changes ΔT of the melted paraffin in the FJ at $W = 3.3 \times 10^5 \text{ W cm}^{-2}$ ($E = 3.7 \text{ J}$, $\tau = 40 \mu\text{s}$, and $D = 6 \text{ mm}$) for $h = 0.4$ (1), 4.4 (2), and 5.4 mm (3).

Table 1 lists the estimates of the temperature T_s of the paraffin melt surface at the end of a laser pulse, which were obtained under assumptions of a complete absorption of the radiation in the near-surface layer and the saturation vapour pressure p for this temperature for $D = 4 \text{ mm}$, $\tau = 40 \mu\text{s}$, $T = 90^\circ\text{C}$, and various E and W . We can see that the FJ appears at a vapour pressure changing over a wide range. It should be noted that the aforementioned transition of the initial stage of FJ evolution from a multiple-jet state to a single jet takes place at a pressure close to atmospheric pressure.

Table 1.

E/J	$W/10^5 \text{ W cm}^{-2}$	T_s/K	p/Torr
0.65	1.3	435	2
1.2	2.4	496	15
1.7	3.4	551	75
2.0	4.0	585	200
2.55	5.1	645	700
3.1	6.2	706	1200
4.0	8.0	806	2050

Note that flows with flooded jets were also obtained at the pulsed irradiation of the surfaces of water, ethanol, kerosene, stearin melt, and glycerin heated up to 160 °C.

4. Properties of flows in the repetitively pulsed mode

When a surface is irradiated in this mode at a laser pulse repetition rate $f > 1/\tau_r$, it can be expected that the flow pattern will differ from that obtained upon irradiation by a single pulse. Because, in actual problems of laser technology, a melt is always bounded by solid walls, the video filming of flows in the repetitively pulsed mode was performed for a limited volume of melted paraffin.

As the pulse repetition rate increases, a radial motion of the melt transforms into a closed flow in the form of two symmetric thermocapillary vortices, which are closed near the focal spot at its edges in the region of the maximum temperature gradient, the pulsating FJ reaches the bottom of the bounding wall, and the liquid transported by the FJ returns to the surface at the periphery of the region adjacent to the FJ. A steady-state flow with an increase in the pulse energy and a constant repetition rate has a similar character: its pattern as a function of energy E is shown in Fig. 4. Despite a deformation of the FJ by the bottom of the bounding wall with increasing E , the thermocapillary vortices hold their shape.

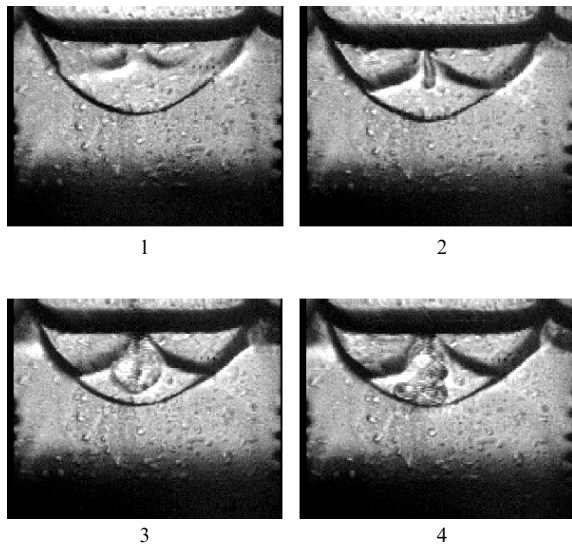


Figure 4. Typical video frames of steady-state flows in a bounded volume of a paraffin melt ($T = 75^\circ\text{C}$) produced by irradiation by laser pulses at $f = 10$ Hz, $\tau = 40$ μs , $D = 4$ mm, and $E = 0.8$ (1), 1.2 (2), 1.5 (3), and 1.9 J (4).

Fig. 5 shows the formation dynamics of a steady-state flow within a bounded volume for a surface irradiated by a train of 50 pulses with $E = 2$ J, $\tau = 40$ μs , and $f = 125$ Hz at $D = 4$ mm. As can be seen, for such radiation parameters, the FJ reaches the bounding wall already in 20 ms, passing a distance of ~ 10 mm, and then is spread over the wall and acquires a resulting form similar to that shown in Fig. 4 (frame 4). As to the radial motion of the melt, the closed vortices pressed against the surface (frame 4 in Fig. 5), which are formed 60 ms after the laser action, reach a lateral wall after another 60 ms (frame 7). Then the vortices

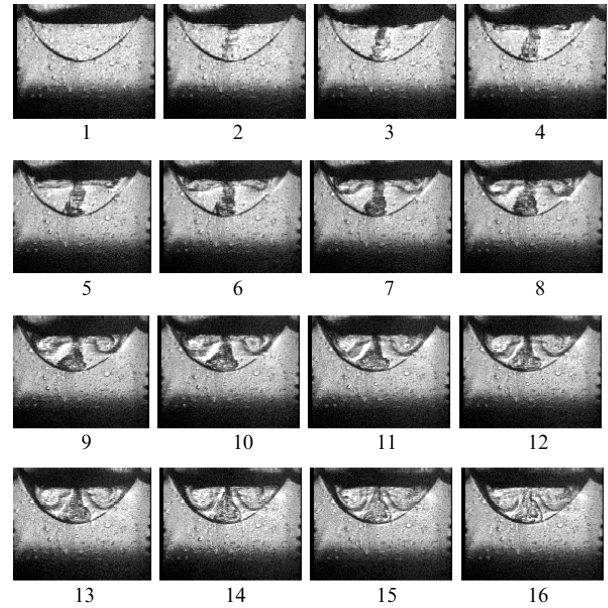


Figure 5. Dynamics of flow formation in a bounded volume of the paraffin melt ($T = 75^\circ\text{C}$) produced by irradiation by a train of 50 laser pulses with $E = 2$ J, $f = 125$ Hz, and $\tau = 40$ μs on the melt surface at $D = 4$ mm. The time interval between the frames is 20 ms.

deepen into the melt and, 240 ms after the start of the irradiation (frame 13), take the form typical of Marangoni vortices.

It should be noted that adding solid cork particles with sizes of $\sim 0.3 - 0.5$ mm and a concentration of $< 10\%$ to the melt during its laser irradiation does not lead to changes in the flow character and parameters. Therefore, the obtained flow characteristics can also be valid for a two-phase medium.

5. Melting of a metal plate irradiated by two lasers

The existence of the FJ and its strong influence on the heat-and-mass transfer, which was shown in model experiments with a paraffin melt, have posed a question of the possibility of similar processes in a metal melt.

For this purpose, supplementary experiments have been performed, in which a stainless steel plate 4 mm thick was irradiated by two laser beams with coinciding centres of the focal spots. A CO_2 laser with a power $P_1 = 3.1$ kW, a focal spot diameter $D_1 = 2.7$ mm, and a controlled duration $\tau_1 = 0.25 - 3$ s of the laser action ensured the target melting for all τ_1 . The radiation of a repetitively pulsed Nd : YAG laser with $f_2 = 50$ Hz, $E_2 = 0.4$ J, $\tau_2 = 100$ μs , and a focal spot diameter $D_2 = 0.8$ or 1.4 mm additionally heated the metal at the irradiation zone up to a temperature exceeding the boiling temperature. The angle between the laser beams was 15° .

The comparison of the melt's metallographic sections obtained at various τ_1 for the irradiation of the plate only by CO_2 laser and for the simultaneous action of two lasers has shown that, despite a slight increase in the average total power $[(P_1 + P_2)/P_1 \approx 1]$, where $P_2 = E_2 f_2 = 20$ W, the melt depth is appreciably larger in the second case. The increase in the melt depth h_m as a function of τ_1 at the simultaneous action of two lasers is shown in Fig. 6. This

effect testifies to the appearance of an additional highly efficient mechanism of heat transfer from the surface to the melt depth. Such a mechanism can be represented by a flow of the FJ type arising in the metal melt under the action of Nd : YAG laser pulses.

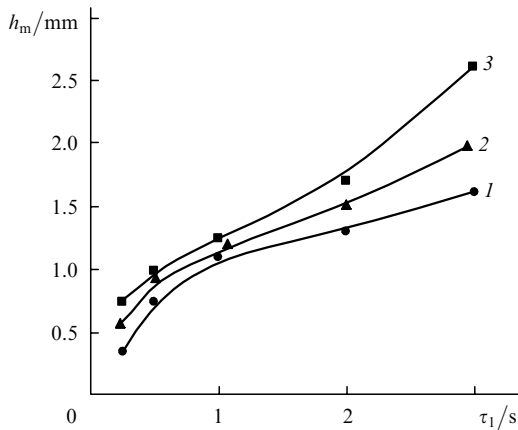


Figure 6. The melt depth h_m as a function of τ_1 under the action of the radiation of (1) only a CO₂ laser and (2, 3) two lasers on the surface of a stainless steel plate 4 mm thick at $D_2 = 1.4$ (2) and 0.8 mm (3).

6. Conclusions

A flow of the FJ type, which was experimentally discovered upon irradiation of a paraffin melt by laser pulses, has a strong effect on the heat and mass transfer and exists in a number of other liquids. The effect of this flow can manifest itself during welding, alloying, hardening accompanied by surface melting, and other technological processes with the application of laser radiation. This is indirectly confirmed by an almost twofold increase in the melt depth upon simultaneous irradiation of a metal surface by two beams from a high-power cw CO₂ laser and a repetitively pulsed Nd : YAG laser with a significantly lower mean radiation power.

Acknowledgements. The authors thank G.G. Gladush for useful discussions of the results of this study. This work was supported by the Russian Foundation for Basic Research (Grant No. 00-02-16161).

References

1. Vedenov A.A., Gladush G.G. *Fizicheskie protsessy pri lazernoj obrabotke materialov* (Physical Processes during Laser Machining of Materials) (Moscow: Energoatomizdat, 1985).
2. Arutyunyan R.V., Baranov V.Yu., Bol'shov L.A., et al. *Vozdeistvie lazernogo izlucheniya na materialy* (Action of Laser Radiation on Materials) (Moscow: Nauka, 1989).
3. Mirzoev F.Kh., Panchenko V.Ya., Shelepina L.A. *Usp. Fiz. Nauk.* **166** (1), 3 (1996).
4. Golubev V.S. *Preprint of IPLIT, Russian Academy of Science* (83) (Shatura, 1999).
5. Gladush G.G., Drobyazko S.V., Likhanskii V.V., et al. *Kvantovaya Elektron.*, **25**, 439 (1998) [*Quantum Electron.*, **25**, 426 (1998)].
6. Chan C.L., Mazumder J., Chen M.M. *Metallurgical Transactions A*, **15**, 2175 (1984).
7. Chan C.L., Chen M.M., Mazumder J. *J. Heat Transfer*, **110** (1), 140 (1988).
8. Tompson M.E., Szekely J. *Int. J. Heat Mass Transfer*, **32**, 1007 (1989).
9. Maiorov V.S., Matrosov M.P. *Kvantovaya Elektron.*, **16**, 806 (1989) [*Sov. J. Quantum Electron.*, **19**, 526 (1989)].
10. Gladush G.G., Likhanskii V.V., Loboiko A.I. *Kvantovaya Elektron.*, **24**, 274 (1997) [*Quantum Electron.*, **27**, 268 (1997)].
11. Likhanskii V.V., Loboiko A.I., Krasnyukov A.G., Antonova G.F., Sayapin V.P. *Kvantovaya Elektron.*, **26**, 139 (1999) [*Quantum Electron.*, **29**, 139 (1999)].
12. Antonova G.F., Gladush G.G., Krasnyukov A.G., Kosyrev F.K., Sayapin V.P. *Teplofiz. Vys. Temp.*, **37**, 865 (1999).
13. Antonova G.F., Gladush G.G., Krasnyukov A.G., Kosyrev F.K., Rodionov N.B. *Teplofiz. Vys. Temp.*, **38**, 501 (2000).
14. Gladush G.G., Drobyazko S.V., Rodionov N.B., Antonova L.I., Senatorov Yu.M. *Kvantovaya Elektron.*, **30**, 1072 (2000) [*Quantum Electron.*, **30**, 1072 (2000)].
15. Gladush G.G., Rodionov N.B. *Kvantovaya Elektron.*, **32**, 14 (2002) [*Quantum Electron.*, **32**, 14 (2002)].